Heterogeneous & Homogeneous & Bio- & Nano-
CHEMCATCHEM
CATALYSIS

Accepted Article

Title: Secondary Impact of Manganese on Catalytic Property of N-Doped Graphene in the Hydrogen Evolution Reaction

Authors: Maryam Bayati and Keith Scott

To be cited as: *ChemCatChem* 10.1002/cctc.201700744

Link to VoR: http://dx.doi.org/10.1002/cctc.201700744

A Journal of
ChemPubSoc Europe

WILEY-VCH

www.chemcatchem.org

WILEY-VCH

COMMUNICATION

Secondary Impact of Manganese on Catalytic Property of N-Doped Graphene in the Hydrogen Evolution Reaction

Maryam Bayati*[a] and Keith Scott[a]

Abstract: Catalysts play a key role in hydrogen production, as a green energy carrier. We have shown for the first time that manganese impurities in graphene can improve the catalytic activity of synthesized N-doped graphene (NG) for the hydrogen evolution reaction in acid media via influencing the ratio of different N-functionalities. This results in a 122 mV improvement in the over-potential following Mn impregnation of graphene. Transmission electron microscopy images confirmed the formation of manganese oxide nanoparticles on NG sheets. X-ray photoelectron spectroscopy revealed structural alteration in favour of higher quantities of quaternary and pyrrolic nitrogen functionalities, from approximately 37% in NG to 84% in Mn-inserted-doped graphene catalyst. This enhanced catalytic performance, based on density functional theory (DFT) calculations in the literature, is attributed to an increase in the number of active sites with higher activity.

Hydrogen is a clean, efficient and green energy carrier which has been pursued to tackle the issues of global warming and also fossil fuel resource depletion by coupling to renewable energy. The major commercial hydrogen production processes; steam reforming and coal gasification with finite resources, have significant impact on carbon emission.The alternative electrochemical methods of hydrogen production although benefits inexpensive, sustainable, abundant and clean precursor of water, are obstructed by employing high-cost and low abundant catalysts of noble metals. As a result, intensive research efforts have been devoted to find and engineer low-cost alternative highly active catalysts such as doped carbon and transition metal compounds; as alloy, oxide, phosphides and sulfides, either as sole or hybrid [1]. Among aforementioned catalysts, heteroatom-doped carbon-based materials exhibit strong tolerance to PH media with high and tunable catalytic activity due to their designable molecular structure which make them a promising candidate[2],[1C],[1G]. Density functional theory (DFT) computations on the nature of the N-doped carbon active sites, which are based on adsorption energies, reaction thermodynamics and activation barriers, elucidated that dopant heteroatoms substantially affect the hydrogen adsorption bond strength on the vicinity carbon atom[2].These calculations showed that carbon next to graphitic and pyrrolic nitrogen,in N-doped catalysts, are more active than the one on pyridinic nitrogen neighborhood [2].Therefore, parameters enhancing the exposed active site number and activity of each site, will increase the activity of the heterogeneous catalyst. Herein, we investigate the impact of Mn impurity,as one of these parameters, on the electro-activity of synthesized N-doped graphene samples by correlating the electrochemical measurements, High resolution transmission electron microscopy (HRTEM) images, X-ray diffraction (XRD), and X-ray photoelectron spectroscopy (XPS) findings of Mn-free and Mn-impregnated samples. Although Mn is not considered as an active catalyst for hydrogen evolution reaction (HER) in acid media [3] and in addition, it is instable in low PH media based on pourbaix diagram. Our findings show that manganese impurities can improve the catalytic activity of nitrogen doped carbon in acid media via influencing the ratio of different N-functionalities. In our experiments, the NG was prepared using Mn-free graphene oxide (GO) (supplementary information) and in a similar procedure, as prepared Mn-inserted nitrogen doped graphene (AP-MnNG), was synthesized by impregnating GO with Mn using potassium permanganate prior to the doping. Finally manganese impurities were removed by soaking in HCl solution and rinsing the solid up to PH neutral (so-called MnNG).

Synthesized catalysts were characterized by a number of microscopic and spectroscopic techniques. Figure 1 presents the XRD pattern of AP-MnNG, MnNG and NG catalysts. As it is demonstrated, the former`s pattern contains manganese oxide features overlaid on N-doped graphene spectra (in MnNG and NG catalysts) as a consequence of impregnating with Mn. AP-MnNG pattern (Figure 1, red line) revealed manganese compounds predominantly as Mn_3O_4 in tetragonal phase (JCPDS No. 00-018-0803), and also MnO in cubic structure(JCPDS No. 04-007-3408). The doped graphene at both spectra showed two significant diffraction peaks at 2θ = 26.5° and 54.6° and an over-lapped peak area between 43 to 44.5°attributed to the (002) and (004) reflections of graphitic carbon, and the over-lapped reflections of C(101) and C(100) planes of a typical turbostratic carbon structure respectively. This implies that the GO was efficiently deoxidized during the hydrothermal process [4]. MnNG catalyst shows no manganese related features, indicates removal of manganese oxides upon reacting with hydrochloric acid (Figure1, blue line).

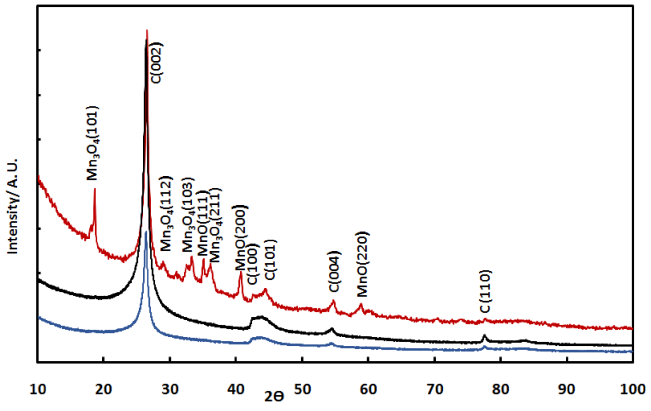

Figure 1. XRD patterns of NG (black line), MnNG (blue line) and AP-MnNG (red line) catalysts.

HRTEM image of NG in low magnification (Figure 2A) revealed a 3D network structure with crumpled layers of N-doped graphene sheets. The high magnification image showed N-doped graphene consisted of few to several layers of graphene, with a lattice spacing of 0.33 nm (Figure 2B). This figure is very close to the one of single-crystal graphene (0.335 nm), representing C(002) and confirming XRD results.

[a] Dr., Maryam, Bayati; Prof., Keith, Scott
CEAM, Newcastle University, Newcastle upon Tyne, UK
E-mail: maryam.bayati@ncl.ac.uk

Supporting information for material synthesis, materials and instrumentation, EDS of AP-MnNG, Raman spectrum, durability test results and the ORCID identification number(s) for authors of the article can be found under:

10.1002/cctc.201700744
WILEY-VCH

COMMUNICATION

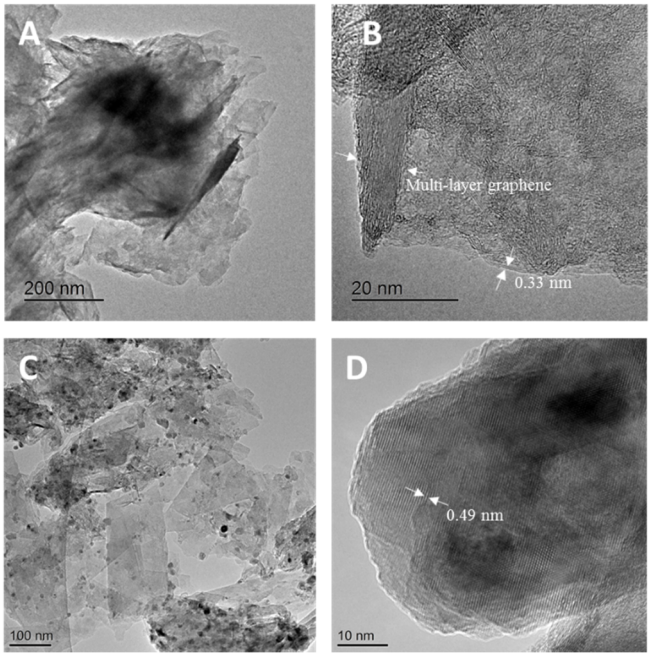

Figure 2. A and B show Low and high magnification HRTEM images of NG respectively. C and D present HRTEM images of AP-MnNG and a manganese oxide nanoparticle in micrograph D, supported on NG respectively.

While the bare NG exhibits a transparent thin layer with homogeneous morphology. AP-MnNG catalyst reveals the 5 to 60 nm size metal oxide layer disperse randomly onto the NG sheet (Figure 2C) as the result of $KMnO_4$ reduction. The high magnification micrgraph (Figure 2D) shows nanoparticles with a lattice spacing of 0.49 nm indexed to the (101) planes of Mn_3O_4(space group = I41/amd) confirming XRD findings. Formation of manganese oxide particles was also confirmed with energy dispersive X-ray spectra (EDS) (Figure S1). XPS measurement was performed to investigate the chemical components of the catalysts.The survey spectra of the catalysts show the characteristic peaks of O1s,C1s and N1s which exhibits incorporation of N atoms in graphene lattice,and with Mn 2p appeared only in AP-MnNG spectra which verifies manganese oxide dissolution by HCl leaching in MnNG compound (Figure 3I). The deconvoluted spectra at Mn region (Figure 3II) displays three pairs of peaks with a spin-orbit splitting of 11.6 eV.The 2P3/2 components located at binding energies of 640.5, 641.8 and 642.8 eV correspond to Mn(II), Mn(III) and Mn(IV) respectively[5] and consistent with XRD results. Figure 3III displays the presence of four deconvoluted peaks of N1s at 398.1, 399.5, 400.3 and 402 eV associated with pyridinic, pyrrolic, graphitic and nitrogen oxide functionalities in NG in agreement with literature [6]. Deconvolution of N1s in AP-MnNG revealed the existence of four nitrogen-containing compounds; pyridinic (397.9), pyrrolic (398.8), quaternary-N (400.3) and N-oxid (402) with red-shift in the position of pyridinic and pyrrolic functionalities (Figure 3III).

To shed light on origin of this shift and the role of central metal, the catalyst was treated by HCl solution and the shift was eliminated in MnNG upon treatment (Figure 3III). While Table1 presents that the N/C ratio remains to a good approximation similar, Table 2 reveal a great change in the quantity of nitrogen functionalities of AP-MnNG, MnNG and NG compounds.

A comparison shows that pyridinic, for NG, and pyrrolic nitrogen for AP-MnNG and MnNG are their main functional groups.The red-shift indicates strong electron interaction between metal and nitrogen as it was observed previously in Mn- and Co-containing N-doped carbon materials [7]. It can be seen from table 2 that the leaching didn`t affect the content of N-components and N/C ratio (Table 1). Moreover, It is known that dicyandiamide and its derivatives act as chelating ligands for Mn [8], and also there is a strong bond between pyrrolic and pyridinic functionalities with Mn in manganese -porphyrin and -Schiff base compounds respectively [9]. These interactions with manganese compound, have been used for growing N-doped carbon materials with thermally-sensitive pyrrole functional group as the dominant N-containing group at elevated temperature of 800 ◦C [10]. It is despite the fact that pyrrolic functional group has less thermal stability in compare to pyridinic and graphitic group and heat treatmentat temperatures above 450 ◦C rearranges it to the latter [11]. Therefore, herein our results show that bonding to Mn in AP-MnNG, protected the pyrrolic group against rearrangement and converting. An asymmetric two-band structure is observed in the O1s spectrum of AP-MnNG. This is resolved into two components corresponding to the binding energies of 530.2 and 532.2 eV, which the former assigned to the lattice oxygen bonding with Mn of manganese oxide[5]. The broad high binding energy peak located at 532.2 eV is attributed to an assembly of carboxylate, carbonyl and hydroxyl at 531.0, 532.3 and 533.7 eV respectively. The removal of Mn upon leaching resulted in eliminating the O1s peak at 530.2 eV from AP-MnNG (Figure 3IV) and left MnNG with the one at higher binding energy, indicates dissolution of manganese oxide components upon acid treatment.

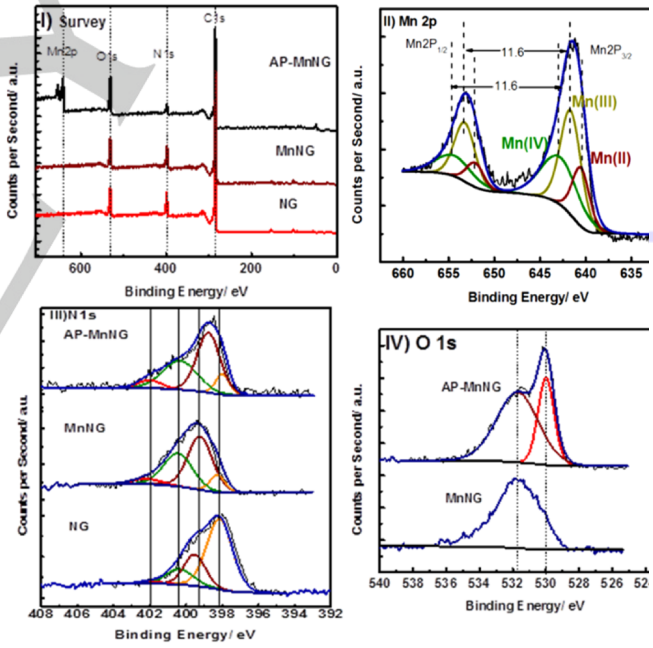

Figure3. I) Survey XPS spectra of NG, MnNG and AP-MnNG, II) Mn 2p region of AP-MnNG, III) N1s region XPS spectra of NG, MnNG and AP-MnNG and IV) O1s region of AP-MnNG and MnNG catalyst.

Table 1. Nitrogen/carbon percentage in NG, MnNG and AP-MnNG catalysts were measured by CHN analyzer and XPS techniques.

Catalysts	NG	AP-MnNG	MnNG
% (N/C) Based on XPS	7.7	7	7.2
% (N/C) Based on CHN	8.1	7.4	7.1

Table 2. Nitrogen functionalities binding energies and their percentages of AP-MnNG, MnNG and NG.

	Binding Energy (eV)/ Fraction (%)		
N-Functional Groups	**AP-MnNG**	**NG**	**MnNG**
Pyridinic	397.9/ 9.88	398.14/ 61.77	398.24/ 9.17
Pyrrolic	398.76/ 48.98	399.52/ 22.65	399.3/ 47.01
Graphitic	400.33/ 34.74	400.35/14.03	400.42/ 38.23
N-O	401.99/ 6.41	402/ 1.55	402.2/ 5.59

Raman spectra have sensitive response to detect the microstructure of the graphene samples.The spectra of NG, MNG and GO samples shown in Figure S2, present two first-order peaks of D and G centered at approximately 1347 and 1600 cm^{-1} respectively. The G band is a first order Raman mode and corresponds to the in-plane, zone center, doubly degenerate phonon mode with E_{2g} symmetry assigned to ordered sp^2 bonded carbon and provides the formation of graphitic carbon. The D band originates from the breathing modes of six-atom rings of κ-point phonons of A_{1g} symmetry corresponds to defects. The peak ratio of I_D/I_G, indicates the level of defects [12] and are 1.18, 1.11 and 1.15 for NG, MNG and GO respectively. Comparing I_D/I_G value to the N-content in NG and MNG (Table 1) shows that a greater N-doping led to a larger defect number and consequently smaller crystallite size. The crystallite size L_a of the nanographite samples was obtained from the integrated intensity ratio I_D/I_G by using Tuinstra and Koenig equation [13] (1) as 14.3, 14.5 and 14.6 nm for NG, MNG and GO respectively. This indicates that the crystallite size domain ,and hence number of grain boundaries, did not change significantly during the synthesis and rejecting the idea of its influence on reactivity of the catalysts.

$$L_a = (2.4 \times 10^{-10})\lambda_L^4 (\frac{I_D}{I_G})^{-1} \quad (1)$$

where the laser excitation wavelength is λ_L (nm).

To evaluate the catalytic behavior of AP-MnNG, MnNG and NG for HER, their linear sweep voltammograms (LSVs) in an aqueous solution of 0.5 M H_2SO_4 were recorded (Figure 4). It can be observed that Pt/C and GO possess the lowest and the highest over-potentials respectively and AP-MnNG presents higher activity than NG. In fact, onset potential reduces from -0.242 V in NG to -0.120 V in AP-MnNG. Knowing that manganese oxide doesn`t show stability and high activity for HER in acid media, it was reasonably deduced that the observed difference in HER activities of AP-MnNG and NG samples originates from the nature of doped functional groups affecting their hydrogen reduction abilities as described theoretically in literature[2]. In addition, to gain further insight into the impact of manganese oxide on overall activity of AP-MnNG, in a control experiment, the LSV of MnNG was recorded. XRD (Figure 1) and XPS spectra of the sample (Figures 3I and 3IV) confirm removal of manganese compounds. As presented in Figure 4, upon etching, the catalytic activity did not diminish and even slightly improved, which can be attributed to removal of nonconductive manganese oxide nanoparticles initially located between N-doped graphene layers. On the basis of these data and the structural information obtained from XRD and XPS data, an explanation for the dramatic shift observed in the HER potential lies within the type and quantity of the active functional groups. According to density functional theory calculations in literatures, the most active sites for HER are carbon in neighborhood of quaternary N configuration in non-edge site followed by carbons in the vicinity of pyrrolic and then pyridinic nitrogen [2].

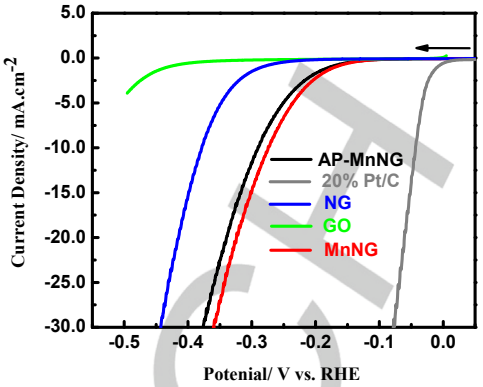

Figure4. Polarization curves of GO (green line), 20% Pt/C (grey line), NG (blue line), AP-MnNG (black line) and MnNG (red line) in N_2 saturated 0.5 M H_2SO_4 solution (scan rate=10 mVs^{-1}). Rotation speed= 1225 rpm.

As it is presented in Table 2,while MnNG and AP-MnNG contain more than 83% graphitic (with >34%) and pyrrolic nitrogen, NG consists of 61% pyridinic and only 36% graphitic (around 14%) and pyrrolic functionalities. Data shows that etching doesn`t influence the amount of various existing functional groups and N/C ratio, therefore it explains the high catalytic activity of the etched sample. Besides, duribility test of MNG catalyst using linear sweep voltammetry (Figure S3) revealed only 15 mV shift at 20 mA cm^{-1} current density after 6000 cycles in 0.5 M sulfuric acid solution, indicating its stability. The stability test ran under same conditions and scan rate of 10 mvs^{-1}.This study reveals the impact of the preparation method on the final structure and activity of the synthesized catalyst as an important factor to take into consideration.

Acknowledgements

This work was financially supported by the EU, NovEED project. Dr. Zabeada Aslam, from University of Leeds for TEM imaging, Dr Jose Portoles for recording XPS spectrum and Mrs. Maggie White from Newcastle University for recording X-ray diffractograms are acknowledged.

Conflict of interest

The authors declare no conflict of interest.

Keywords: Mn insertion• N-doped Graphene• Hydrogen evolution reaction• Catalyst•

[1] A) M. Gong, W. Zhou, M. C. Tsai, J. Zhou, M. Guan, M. C. Lin, B. Zhang, Y. Hu, D. Y. Wang, J. Yang, S. J. Pennycook, B. J. Hwang, H. Dai, "Nanoscale nickel oxide/nickel heterostructures for active hydrogen evolution Electrocatalysis" *Nat. Commun.***2014**, *5*, 4695.B) Z. W. She, J. Kibsgaard, C. F. Dickens, I. Chorkendorff, J. K. Nørskov, T. F. Jaramillo, "Combining theory and experiment in electrocatalysis: Insights into materials design" Science **2017**, DOI: 10.1126/science.aad4998. C) X. Zouc, Y. Zhang, "Noble metal-free hydrogen evolution catalysts for water splitting" *Chem. Soc. Rev.***2015**,44, 5148-5180.D) Z. Xing, Q. Liu, A. M. Asiri, X. Sun, "Closely interconnected network of molybdenum phosphide nanoparticles: a highly efficient electrocatalyst for generating hydrogen from water" *Adv. Mater.***2014**, *26,* 5702−5707.E) Q. Lu, G. S. Hutchings, W. Yu, Y. Zhou, R. V. Forest, R. Tao, J. Rosen, B. T. Yonemoto, Z. Cao, H. Zheng, J. Q. Xiao, F. Jiao, J. G.Chen, "Highly porous non-precious bimetallic electrocatalysts for efficient hydrogen evolution" *Nat. Commun.***2015**, 6:6567, doi:10.1038/ncomms7567.F) D. R. Cummins, U. Martinez, A. Sherehiy, R. Kappera, A. Martinez-Garcia, R. K. Schulze, J.

Jasinski, J. Zhang, R. K. Gupta, J. Lou, M. Chhowalla, G. Sumanasekera, A. D. Mohite, M. K. Sunkara, G. Gupta, "Efficient hydrogen evolution in transition metal dichalcogenides via a simple one-step hydrazine reaction" Nat. Commun. **2016**, 7, 11857 doi:10.1038/ncomms11857.G) G. Zhu, L. Ma, H. Lv, Y. Hu, T. Chen, R. Chen, J. Liang, X. Wang, Y. Wang, C. Yan, Z. Tie, Z. Jin, J. Liu, "Pine needle-derived microporous nitrogen-doped carbon frameworks exhibit high performances in electrocatalytic hydrogen evolution reaction and supercapacitors" *Nanoscale*, **2017**,*9*, 1237-1243.H) Y. Ito, W. Cong, T. Fujita, Z. Tang, M. Chen, "High catalytic activity of nitrogen and sulfur Co-doped nanoporous graphene in the hydrogen evolution reaction" *Angew. Chem. Int. Ed.* **2015**, *54*, 2131 –2136.I) Y. Liu, H. Yu, X. Quan, S. Chen, H. Zhao, Y. Zhang, "Efficient and durable hydrogen evolution electrocatalyst based on nonmetallic nitrogen doped hexagonal carbon" *Sci. Reports***2014**, *4*, Article number: 6843 doi:10.1038/srep06843.

[2] A) H. Dong, C. Liu, H. Ye, L. Hu, B. Fugetsu, W. Dai, Y. Cao, Qi, X. H. Lu, X. Zhang"Three-dimensional nitrogen-doped graphene supported molybdenum disulfide nanoparticles as an advanced catalyst for hydrogen evolution reaction" *Scientific Reports***2015**, doi:10.1038/srep17542.B)Y. Zheng,Y. Jiao,L. H. Li, T. Xing, Y. Chen, M. Jaroniec, S. Z. Qiao "Toward Design of Synergistically Active Carbon-Based Catalysts for Electrocatalytic Hydrogen Evolution" *ACS Nano*, **2014**, *8*, 5290–5296.C) Y. Jiao, Y. Zheng, K. Davey, S-Z Qiao,"Activity origin and catalyst design principles for electrocatalytic hydrogen evolution on heteroatom-doped graphene" *Nat. Energy***2016**, 1, 16130-16136.

[3] A. Morozan, V. Goellner, Y. Nedellec, J. Hannauer, F. Jaouen "Effect of the Transition Metal on Metal–Nitrogen–Carbon Catalysts for the Hydrogen Evolution Reaction" *J. Electrochem. Soc.*, **2015**,*162*, H719-H726.

[4] A) Y. Zou, I. A. Kinloch, R. A. W. Dryfe,"Mesoporous Vertical Co3O4 Nanosheet Arrays on Nitrogen-Doped Graphene Foam with Enhanced Charge-Storage Performance " *ACS Appl. Mater. Interfaces***2015**, *7*, 22831−22838.B) Z.Q. Li, C.J. Lu, Z.P. Xia, Zhou, Y.; Z. Luo"X-ray diffraction patterns of graphite and turbostratic carbon" *Carbon*, **2007**, *45*, 1686–1695.

[5] Q. Tang, L. Jiang, J. Liu, S. Wang, G. Sun,"Effect of surface manganese valence of manganese oxides on the activity of the oxygen reduction reaction in alkaline media" *ACS Cata*.**2014**, *4*, 457-463.

[6] M. Bayati, K. Scott,"Synthesis and Activity of A Single Active Site N-doped Electro-catalyst for Oxygen Reduction"*Electrochim. Acta***2016**, *213*, 927-932.

[7] A) Y. Xiao, X. Wang, W. Wang, D. Zhao, M. Cao, "Engineering hybrid between MnO and N‐doped carbon to achieve exceptionally high capacity for lithium-ion battery anode" *ACS Appl. Mater. Interfaces* **2014**, *6*, 2051-2058.B) Z., J. Jiang, Z. Jiang, "Interaction induced high catalytic activities of CoO nanoparticles grown on nitrogen-doped hollow graphene microspheres for oxygen reduction and evolution reactions" *Sci. Rep.***2016**, *6*, doi: 10.1038/srep27081.

[8] A) A. Igashira-Kamiyama, T. Kajiwara, M. Nakano, T. Konno, T. Ito,"Syntheses, structures, and magnetic properties of tetramanganese(III) and hexamanganese(III) complexes containing derivative of biguanidate ligand: ferromagnetic interaction via iminonitrogen" *Inorg. Chem.*, **2009**, *48*, 11388–11393.B) L. J. Boucher, K. Koeber, M. Kotowsky, D. *Chemical Handbook of Inorganic Chemistry Mn Coordination Compounds*, Springer-Verlag Edition 7 D5, **1987**, PP.158.

[9] M. Kurihara, K. Ozutsumi, T. Kawashima "Complexation of manganese(II) and zinc(II) ions with pyridine, 3-methylpyridine and 4-methylpyridine in dimethylformamide" *J. Chem. Soc., Dalton Trans.,***1993**, *22*, 3379-3382.

[10] Y. Tan, C. Xu, G. Chen, Z. Liu, M. Ma, Q. Xie, N. Zheng, S. Yao, " Synthesis of Ultrathin Nitrogen-Doped Graphitic Carbon Nanocages as Advanced Electrode Materials for Supercapacitor*" ACS Appl. Mater. Interfaces* **2013**, *5*, 2241−2248.

[11] A) R. Arrigo, M. Hävecker, R. Schlögl, D.S. Su,"Dynamic surface rearrangement and thermal stability of nitrogen functional groups on carbon nanotubes" *Chem. Commun*.**2008**, 4891–4893.B) H. Schmiersa, J. Friebela, P. Streubelb, R. Hesseb, R. Köpsela, " Change of chemical bonding of nitrogen of polymeric N-heterocyclic compounds during pyrolysis" Carbon,**1999**, *37*, 1965 –1978. C) M. Scardamaglia, B. Aleman, M. Amati, C. Ewels, P. Pochet, N. Reckinger, J.F. Colomer, T. Skaltsas, N. Tagmatarchis, R. Snyders, L. Gregoratti, C. Bittencourt,"Nitrogen implantation of suspended graphene flakes: annealing effects and selectivity of Sp2 nitrogen species" Carbon **2014**,*73*, 371–381.D) B. Xiao, J. P. Boudou , K. M. Thomas,"Reactions of nitrogen and oxygen surface groups in nanoporous carbons under Inert and reducing atmospheres" Langmuir, **2005**, *21*, 3400–3409.

[12] Q. Shi, Y. Wang , Z. Wang, Y. Lei, B. Wang, N. Wu, C. Han, S. Xie, Y. Gou, „Three-dimensional (3D) interconnected networks fabricated via in-situ growth of N-doped graphene/carbon nanotubes on Co-containing carbon nanofibers for enhanced oxygen reduction" *Nano Research*, **2016**, *9*, 317-328.

[13] F. Tuinstra, J. L. Koenig, „Raman spectrum of graphite*" J. Chem. Phys.* **1970**, *53*, 1126–1130.

WILEY-VCH

COMMUNICATION

Entry for the Table of Contents (Please choose one layout)

Layout 1:

COMMUNICATION

Text for Table of Contents

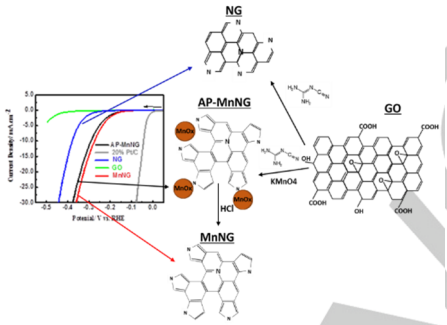

Maryam Bayati, Keith Scott*

Page No. – Page No.
Secondary Impact of Manganese on Catalytic Property of N-Doped Graphene in the Hydrogen Evolution Reaction

Layout 2:

COMMUNICATION

Text for Table of Contents

*Author(s), Corresponding Author(s)**

Page No. – Page No.

Title